Multi-User Aware Frame Structure for OFDMA Based System

Alphan Şahin*, *Student Member, IEEE,* and Hüseyin Arslan†, *Senior Member, IEEE,*
University of South Florida, Tampa, FL, 33620 Emails: alphan@mail.usf.edu*, arslan@usf.edu†

***Abstract*—In this paper, we propose a multi-user aware frame structure for doubly dispersive channels in order to increase both spectral efficiency and frequency spread immunity of orthogonal frequency division multiple accessing (OFDMA) based systems. Unlike the conventional OFDMA based system where the fixed cyclic prefix duration and subcarrier spacing are utilized within the frame structure considering the worst case communication channel, in the proposed approach, multiple cyclic prefix durations and subcarrier spacings are employed. In order to build the proposed frame structure, the statistics of the mobility and the range of the users are mapped to inter-carrier-interference and maximum excess delay to obtain multiple subcarrier spacings and cyclic prefix durations. As a result, better frequency spread immunity and spectral efficiency are achieved by exploiting the doubly dispersive channel characteristics of the users.**

***Index Terms*—Cyclic prefix, delay spread, frequency spread, frame structure, OFDMA, subcarrier spacing.**

I. Introduction

Efficient usage of the electrospace with orthogonal frequency division multiple accessing (OFDMA) based waveforms has gained an extra importance with the recent advances in wireless communication e.g. white space radios and 4G technologies [1]–[3]. One of the fundamental reasons of this attraction is the fact that OFDMA offers a flexible structure which exploits the three dimensions of the electrospace (time, frequency, and spatial domains) very efficiently. In this paper, our focus is the exploitation of time and frequency domains further. Depending on the channel characteristics of the users, these two dimensions might be exposed to the different time and frequency responses at the same time which is also known as doubly dispersive channel. We exploit having multiple users with different doubly dispersive channels by adapting the time-frequency structure of OFDMA scheme.

A large number of parameters (e.g. number of active subcarriers, location of pilot subcarriers, windowing size etc.) are related with the time-frequency structure of OFDMA symbol. Among many others, subcarrier spacing (Δf) and cyclic prefix duration ($T_{\rm CP}$) are the two fundamental parameters that determine the time-frequency structure of OFDMA symbol. Subcarrier spacing Δf, thereby the OFDMA symbol duration ($T_{\rm s}=1/\Delta f$), is related with both frequency spread and delay spread characteristics of the channel. As a rule of thump, the lower limit of Δf determined with the coherence time. On one hand, a wider Δf is desired to tolerate the inter-carrier-interference (ICI), on the other hand, decreasing Δf would be helpful to increase the spectral efficiency. Also, Δf indirectly impacts $T_{\rm CP}$, since $T_{\rm CP}$ depends on the delay spread characteristics of the channel. While longer $T_{\rm CP}$ is desirable to avoid inter-symbol-interference (ISI) between OFDMA symbols, employing short $T_{\rm CP}$ increases the spectral efficiency.

Consider a frame which consists of multiple OFDMA symbols as in Fig.1. In the conventional frame structures, Δf and $T_{\rm CP}$ are set to certain values considering the worst case channel scenario supported by the system. In other words, fixed $T_{\rm CP}$ and Δf are used within the frame, as long as the orthogonality between subcarriers is provided sufficiently for the worst case channel scenario. However, this approach does not exploit having multiple users with different doubly dispersive channel characteristics. For example, it does not consider the users which have less maximum excess delays than the worst maximum excess delay spread ($T_{\max}$) like nearby users to the base station [4]. Also, it does not employ narrower Δf to reduce the redundancy for stationary users.

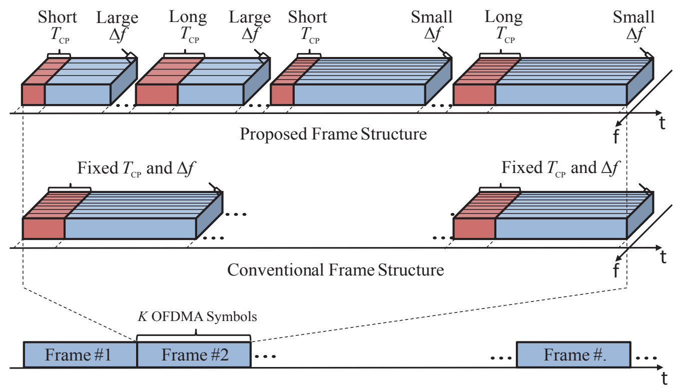

Fig. 1: Conventional and proposed frame structures in time and frequency domains.

In literature, it is possible to find several adaptation methods on time-frequency structure of OFDMA symbol. In [5], adaptation on $T_{\rm CP}$ is investigated for orthogonal frequency division multiplexing (OFDM) based systems. After the transmitter estimates the root-mean-square delay spread ($T_{\rm rms}$) of the channel, $T_{\rm CP}$ is adaptively selected as twice of the estimated $T_{\rm rms}$ of the channel as a rule of thumb. Asserting the delay spread criterion is not sufficient to select $T_{\rm CP}$, the system capacity is given as a function of $T_{\rm CP}$ and signal-to-noise ratio (SNR) in [6]. Based on the analysis of the distribution of the capacity, $T_{\rm CP}$ is investigated for the IEEE 802.11 channel models for the distances between 3 m and 60 m. In their following studies, the joint allocation of the power and $T_{\rm CP}$ is considered to maximize the system capacity [7] and the optimal criterion for the capacity is given to adapt $T_{\rm CP}$ considering the power line communication systems [8]. However, as indicated in [9], the approaches in [6]–[8] rely on given values of $T_{\rm rms}$. Therefore, being aware of the importance of the statistical knowledge of the $T_{\rm rms}$, an adaptation scheme based on a priori knowledge of the channel statistics is suggested to reduce feedback requirements in [9]. Employing the prior statistics of $T_{\rm rms}$, $T_{\rm CP}$ is optimized considering the system capacity. In [10], Δf is dynamically changed for each OFDMA frame to increase the throughput. However, using different Δf for each frame changes the frame duration and increases the complexity of initial accessing and synchronization algorithms. Also, if all users are mapped into the frame, performances of the users cannot be optimized with frame-to-frame adaptation. For in-frame adaptation, a reconfigurable mixed frame structure is introduced to maintain the gain provided by the band-adaptive modulation and coding (Band-AMC) under the large delay spread scenarios in [11]. The users are scheduled to the subcarriers when the band-AMC mode has no gain over the diversity mode based on the frequency selectivity of the user within the frame. Also, some adaptations on T_{CP} and Δf are employed in LTE and WiMaX, even if these standards are based on fixed T_{CP} and Δf within the frame. For example, T_{CP} is adaptive from one base station to another one in LTE and WiMAX systems. For example, short T_{CP} (4.69 μs) and long T_{CP} (16.6 μs) are used for small and large cells respectively, on the condition that fixed T_{CP} within the cell is utilized. Also, different Δf options are allowed in fixed WiMAX by keeping Δf fixed for all users within a frame. In order to cope with signal-to-interference-plus-noise ratio (SINR) degradation due to the mobility, general approach is to change the coding rate and modulation order adaptively instead of Δf. The number of subcarriers per unit bandwidth is doubled only for broadcasting scenarios in order to avoid the overhead arising from the cyclic prefix in LTE [2, p. 330]. Also, the reader can find the required SINR and modulation order in [12, p. 221] for a given mobile speed (v) to obtain the desired spectral efficiency. As can be seen from the literature, even if the studies are aware of the advantage of the variation of the user channel characteristics, to best of our knowledge, having multiple OFDMA symbols with multiple cyclic prefix durations and subcarrier spacings within the frame is not investigated statistically in the literature.

In this paper, we propose doubly dispersive channel adaptive frame structure for OFDMA based systems as shown in Fig.1. Multiple T_{CP} and Δf within the frame are employed to provide the adaptations to the doubly dispersive channels of the users. While multiple T_{CP} within a frame are utilized considering the distances between the users and the base station, multiple Δf within the frame are used to increase to the frequency spread immunity of the users considering their mobility characteristics. The proposed user aware frame structure is investigated with the statistical approaches.

The paper is organized as follows. The proposed frame structure is introduced in Section II. Determining the parameters of the proposed frame structure with statistical approaches is investigated in Section III. An example design is presented is Section IV. Finally, the paper is concluded in Section V.

II. Proposed Frame Structure

Proposed frame structure exploits different doubly dispersive channels of the users in the cell. In other words, as the users have different delay spread and mobility characteristics in the cell, employing multiple T_{CP} and Δf would be beneficial in terms of the spectral efficiency and the frequency spread immunity of the users.

Critically important that T_{rms} is related with the distance between the user and the base station statistically. The mathematical expression relating T_{rms} with a certain distance is proposed in [4] as

$$T_{\text{rms}} = T_1 r^{\epsilon} y \tag{1}$$

where r is the distance between the base station and the user in kilometers, ϵ is a distance coefficient lies between $0.5 \leq \epsilon \leq 1$, T_1[1] is the median value of T_{rms} at r = 1 km, and y is a lognormal distributed random variable as

$$f_y\left(y\right) = \frac{\xi}{\sigma_y y \sqrt{2\pi}} \mathrm{e}^{-\frac{(10\log_{10} y)^2}{2\sigma_y^2}}. \tag{2}$$

[1]Note that even if T_1 is given as a constant in [4], its value changes for a given cell type e.g. the urban microcells (0.4 μs) and urban macrocell (0.4 μs-1 μs). This change on T_1 is in favor of the proposed frame structure in terms spectral efficiency increment compared to fixed frame structure. For the sake of sticking to the proposed model in [4], T_1 is considered as a constant.

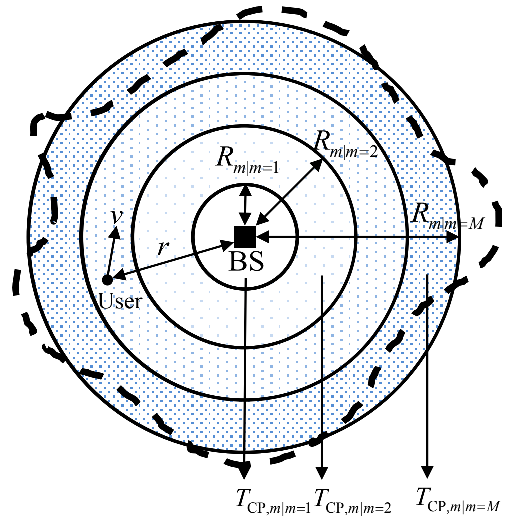

Fig. 2: Cyclic prefix durations in the proposed frame structure are calculated by dividing the cell with circles.

In (2), ξ is $10/\ln(10)$ and σ_y is the standard deviation of y which lies as $2 \leq \sigma_y \leq 6$ in dB depending on the environment. If we assume the power delay profile of the channel decays exponentially, using the equations given in [13], the relationship between $T_{\max}$ and T_{rms} is obtained as $T_{\max} \cong \ln(X) T_{\text{rms}}$ where X shows the fall in linear scale relative to the maximum tap power. For example, if $X = 20$ dB, $T_{\max}$ is approximately expressed as $T_{\max} \cong 5T_{\text{rms}} = 5T_1 r^{\epsilon} y$. Thus, we can interpret that if the distance between the user and the base station increases, higher $T_{\max}$ values are expected. Hence, if the cell is divided into M inner circles with the radius of R_m where $m = 1, 2, ..., M$ as in Fig.2, the sufficient cyclic prefix duration ($T_{\text{CP},m}$) for each area between consecutive inner circles is calculated statistically for a given confidence limit (γ_{CP}). The confidence limit basically gives a probability for selected cyclic prefix duration which is longer than γ_{CP} of the $T_{\max}$ variation and it is between 0 and 1. For example, $T_{\text{CP},m}$ can be selected as high as to cover 90% of the $T_{\max}$ variation (which means $\gamma_{\text{CP}} = 0.9$) for given R_{m-1} and R_m. Note that since $T_{\text{CP},m} \leq T_{\text{CP},M}$, the spectral efficiency of the system will increase compared to the conventional frame structure. In addition to using different cyclic prefix durations, L multiple subcarrier spacings (Δf_ℓ) are employed within the frame where $\ell = 1, 2, ..., L$. Considering the different mobility characteristics of the users, Δf_ℓ is determined for given confidence limit ($\gamma_{\Delta f}$), carrier frequency (f_{c}), and tolerable ICI power (P_{ICI}). Similar to γ_{CP}, $\gamma_{\Delta f}$ indicates Δf_ℓ which supports $\gamma_{\Delta f}$ portion of the users at different speeds in the cell and it lies between 0 and 1.

The number of OFDMA symbols with $T_{\text{CP},m}$ and Δf_ℓ are determined using the distributions of r and v of the users belonging to the base station, respectively. Consider that K OFDMA symbols are transmitted in the frame. The number of OFDMA symbols with same $T_{\text{CP},m}$ and the number of OFDMA symbols with same Δf_ℓ within the frame are calculated as $K_m = \rho_m K$ and $K_\ell = \rho_\ell K$, respectively. While ρ_m represents the ratio of the number of the users located in the area between the circles with R_m and R_{m-1} to the total number of users in the cell, ρ_ℓ is the probability of the covered speed variation in the cell where generated ICI is less than P_{ICI} between Δf_ℓ and $\Delta f_{\ell-1}$. Also, each group of OFDMA symbol with the same $T_{\text{CP},m}$ and Δf_ℓ is determined as $K_{m,\ell} = \rho_m \rho_\ell K$.

The duration of the proposed frame structure is less than the conventional frame structure since the proposed frame reduces the redundant cyclic prefix usage. The increment on the spectral efficiency (ΔR) compared to the conventional frame structure with the same design criteria (i.e. bandwidth, P_{ICI}, γ_{CP} and $\gamma_{\Delta f}$) are calculated in percent as

$$\Delta R = \left[\sum_{\ell=1}^{L} \frac{100 \rho_\ell \left(1 + \Delta f_L T_{\mathrm{CP},M}\right)}{1 + \sum_{m=1}^{M} \rho_m \Delta f_\ell T_{\mathrm{CP},m}} \right] - 100 \ . \qquad (3)$$

III. Determining the Parameters of the Proposed Frame Structure

In this section, the selections of the parameters of the proposed frame structure are investigated. Firstly, the distributions of $T_{\max}$ and r are investigated to determine $T_{\mathrm{CP},m}$ and ρ_m, respectively. Then, the distributions of mobility in the cell is investigated to obtain Δf_ℓ and ρ_ℓ.

A. Determining $T_{\mathrm{CP},m}$ and ρ_m

In order to use multiple cyclic prefix durations within the frame structure properly, cumulative distribution function (CDF) of $T_{\max}$ should be calculated for a given R_m and R_{m-1}. In order to calculate the distribution of r for a given area between consecutive circles, we rewrite (1) as

$$T_{\max} \cong \ln(X) T_1 r^{\epsilon} y = k r^{\epsilon} y \qquad (4)$$

for the sake of generalization for $T_{\max}$. If we assume that the user density is uniform in the area between the consecutive inner circles, probability density function (PDF) of r is obtained as

$$f_r(r) = \frac{2r}{R_m^2 - R_{m-1}^2}. \qquad (5)$$

We should indicate that the user density might be different in the cell. If the difference between R_m and R_{m-1} is relatively small to R, the user density in the area of the consecutive inner circles can be assumed as uniform. Therefore, considering PDF given in (5) would be approximately correct for other practical user densities i.e. Gaussian and exponential.

Applying the rule of function of a random variable and derivations for PDF of T_{rms} in [4], PDF of $T_{\max}$ is found as

$$f_{T_{\max}}(T_{\max}) = \frac{\mathrm{e}^{\frac{2\sigma_y^2}{\xi^2\epsilon^2}} T_{\max}^{\frac{2}{\epsilon}-1} \ \mathrm{erf}\Big|_{\frac{10}{\sqrt{2}\sigma_y}\log_{10}\left(\frac{T_{\max}}{kR_m^{\epsilon}}\right)+\frac{\sqrt{2}\sigma_y}{\xi\epsilon}}^{\frac{10}{\sqrt{2}\sigma_y}\log_{10}\left(\frac{T_{\max}}{kR_{m-1}^{\epsilon}}\right)+\frac{\sqrt{2}\sigma_y}{\xi\epsilon}}}{\epsilon k^{\frac{2}{\epsilon}}\left(R_m^2 - R_{m-1}^2\right)} \qquad (6)$$

where $\mathrm{erf}|_{\mathrm{b}}^{\mathrm{a}} = \mathrm{erf}(\mathrm{a}) - \mathrm{erf}(\mathrm{b})$ and $\mathrm{erf}(\cdot)$ is Gaussian error function. Integrating (6), closed-form CDF of $T_{\max}$ is obtained as

$$\mathrm{F}_{T_{\max}}(T_{\max}) = \frac{1}{2} - \frac{\mathrm{e}^{\frac{2\sigma_y^2}{\xi^2\epsilon^2}} T_{\max}^{\frac{2}{\epsilon}} \left[\Lambda(T_{\max}, R_m) - \Lambda(T_{\max}, R_{m-1})\right]}{2k^{\frac{2}{\epsilon}}\left(R_m^2 - R_{m-1}^2\right)} \qquad (7)$$

where

$$\Lambda(T_{\max}, Z) = \mathrm{erf}\left(\frac{10}{\sqrt{2}\sigma_y}\log_{10}\left(\frac{T_{\max}}{kZ^{\epsilon}}\right) + \frac{\sqrt{2}\sigma_y}{\xi\epsilon}\right) - e^{-\frac{2\sigma_y^2}{\xi^2\epsilon^2}} \left(\frac{T_{\max}}{kZ^{\epsilon}}\right)^{-\frac{2}{\epsilon}} \mathrm{erf}\left(\frac{10}{\sqrt{2}\sigma_y}\log_{10}\left(\frac{T_{\max}}{kZ^{\epsilon}}\right)\right). \qquad (8)$$

Therefore, $T_{\mathrm{CP},m}$ is calculated as

$$\mathrm{F}_{T_{\max}}(T_{\mathrm{CP},m}) \geq \gamma_{\mathrm{CP}} \qquad (9)$$

using (7) for given T_1, R_m, R_{m-1} and γ_{CP}.

In order to calculate the number of OFDMA symbols with the same cyclic prefix duration within the frame, the probability of having of a user being in the area between consecutive circles should be calculated. Once it is obtained via CDF of r for given R_m and R_{m-1}, ρ_m is obtained by calculating

$$\rho_m = \mathrm{F}_r(R_m) - \mathrm{F}_r(R_{m-1}) \qquad (10)$$

for every m.

Heuristically, we assume that geographical user distribution is uniform in the area. However, note that even if the geographical user density is uniform, the users linked to the corresponding base station might not be uniform depending on the overlapping cell scenarios and shadowing characteristics of the environment [14]. In order to obtain a realistic user distance distribution, the methodology introduced in [14] is followed. In the geographical environment, average path loss and shadowing are modeled as $\overline{L}(\cdot) = A + B\log_{10}(\cdot)$ and lognormal distribution with σ standard variation, respectively. K base stations with equal transmission power (P_{tx}) are deployed at (r_k, θ_k) coordinates with equal distance (L_{d}). Additionally, the users are shared between base stations according to the received signal strength indicator (RSSI) measurements. Therefore, by defining the link probability between a user located at (r, θ) and kth base station as

$$\mathcal{P}_k(r, \theta) = \frac{1}{2} - \frac{1}{2}\mathrm{erf}\left(\frac{P_{\min} + \Delta - P_{\mathrm{tx}} + \overline{L}(d_k(r, \theta))}{\sqrt{2}\sigma}\right)$$

where $P_{\min}$ is the receiver sensitivity, Δ is the handover margin [15, Ch. 2], $d_k(r, \theta) = \sqrt{r^2 + r_k^2 - 2rr_k\cos(\theta - \theta_k)}$ is the distance between user and kth base station, the distribution of r is given as

$$f_r(r) = \frac{\int_0^{2\pi} \mathbf{P}(r, \theta) r d\theta}{\int_0^{\infty}\int_0^{2\pi} \mathbf{P}(r, \theta) r d\theta dr} \qquad (11)$$

where

$$\mathbf{P}(r, \theta) = \sum_{i=1}^{K} \gamma(r, \theta) \mathcal{P}_1(r, \theta) \mathbf{C}_{i-1}(r, \theta) \ , \qquad (12)$$

$$\mathbf{C}_x(r, \theta) = \sum_{\forall \mathcal{L} \in \mathcal{K}_x} \prod_{\substack{l \in \mathcal{L} \\ m \in \mathcal{L}^c}} \mathcal{P}_l(r, \theta)(1 - \mathcal{P}_m(r, \theta)) \ . \qquad (13)$$

In (12) and (13), $\mathbf{P}(r, \theta)$ is the probability of establishing a link between a user located at (r, θ) to the $(k = 1)$th base station considering all other deployed base stations, i is the sharing index, $\gamma(r, \theta)$ is the user sharing function which is suggested as the ratio of the received signal power from $(k = 1)$th base station to the summation of the received signal powers from all base stations for RSSI based sharing, $\mathbf{C}_x(r, \theta)$ is the probability of observing x base stations (excluding $(k = 1)$th base station) which can provide power more than $P_{\min} + \Delta$ at the receiver, $\mathcal{K}_x$ is the set of index subset generated with x-combinations of $\{2, ..., K\}$, $\mathcal{L}$ and $\mathcal{L}^c$ are index set and complementary index set, respectively. By evaluating the integration of (11), it is possible to solve (10) for the sake obtain realistic ρ_m values.

B. Determining Δf_ℓ and ρ_ℓ

In the literature, the mobility of the user is modeled with several PDFs e.g. beta distribution [16] and Rice-plus-normal distribution [17] including both urban streets and major roads. It is possible to find mobility models which also take the car stops at crossroads [18] and different the street patterns [19] into account. Since the suggested mobility model in [17] includes the validation with measurements, we consider the mobility model which is given as

$$f_v\left(v\right) = (1-p_{\rm road})\frac{v}{\sigma_v^2}{\rm e}^{-\frac{v^2+\bar{v}_{\rm city}^2}{2\sigma_v^2}} I_0\left(\frac{v\bar{v}_{\rm city}}{\sigma_v^2}\right) + p_{\rm road}\frac{1}{\sigma_v\sqrt{2\pi}}{\rm e}^{-\frac{(v-\bar{v}_{\rm road})^2}{2\sigma_v^2}} \quad (14)$$

where $p_{\rm road}$ is the probability of cars on the major roads, $\bar{v}_{\rm city}$ is the mean speed in the city, $\bar{v}_{\rm road}$ is the mean speed of the major-road traffic, σ_v is the deviation of the speed, and $I_0\left(.\right)$ is the modified Bessel function of the first kind with order zero. Integrating (14), CDF of v is obtained as

$$\mathrm{F}_v\left(v\right) = \left(1-p_{\rm road}\right)\left[1-Q_1\left(\frac{\bar{v}_{\rm city}}{\sigma_v},\frac{v}{\sigma_v}\right)\right] + p_{\rm road}\left[1-Q\left(\frac{v-\bar{v}_{\rm road}}{\sigma_v}\right)\right] \quad (15)$$

where $Q_1\left(\cdot,\cdot\right)$ is the Marcum Q-function [20] and $Q\left(\cdot\right)$ is the Q-function.

Universal upper bound of the relative ICI power leaking from the normalized signal power due to the mobility is given by [21]

$$P_{\rm ICI} \leq \frac{1}{12}\left(2\pi\frac{f_{\rm d}}{\Delta f}\right)^2 = \frac{1}{12}\left(2\pi\frac{vf_{\rm c}}{c\Delta f}\right)^2 \quad (16)$$

where $f_{\rm d}$ is the maximum Doppler shift and c is the speed of the light. Therefore, combining (15) and (16), CDF of Δf is derived as

$$\mathrm{F}_{\Delta f}\left(\Delta f\right) = \mathrm{F}_v\left(v = \frac{\sqrt{3P_{\rm ICI}}}{\pi\frac{f_{\rm c}}{c\Delta f}}\right). \quad (17)$$

Using (17), Δf_L is obtained as

$$\mathrm{F}_{\Delta f}\left(\Delta f_L\right) \leq \gamma_{\Delta f}. \quad (18)$$

Since each selected Δf_ℓ indicates a speed limit on the curve of $\mathrm{F}_{\Delta f}\left(\Delta f_L\right)$ for a given $P_{\rm ICI}$, ρ_ℓ is found as

$$\rho_\ell = \mathrm{F}_{\Delta f}\left(\Delta f_\ell\right) - \mathrm{F}_{\Delta f}\left(\Delta f_{\ell-1}\right). \quad (19)$$

IV. A Design Example

A design example is given in order to compare analytical findings with simulations and to investigate the performance of proposed frame structure. An urban environment where the path loss characteristics is modelled as *Urban Macro (UMa)* with the parameters given in [22] is taken into account. Operating frequency is set to 2 GHz. Thus, the path loss parameters are obtained as $A = 19.6$ and $B = 39$, and $\sigma = 4$ dB. The channel scattering in time is modeled with exponential decaying power delay profile where $X = 20$ dB. In addition, ϵ, σ_y and T_1s are selected as 0.5, 2 dB, and 0.41μs, respectively [4]. In the area, 7 base stations are deployed considering hexagonal tessellation where $L_{\rm d} = 2400$ m. Also, Δ and $P_{\rm tx}$ is set to 4 dB and 36 dBm, respectively. The frame structure is generated with $K = 140$ OFDMA symbols. In order to construct the frame structure of the center base station, we divide the cell into $M = 5$ circles where $R_{m|m=1,2,\ldots,5} = [0.3,\ 0.6,\ 0.9,\ 1.2,\ 1.5]$ in kilometers.

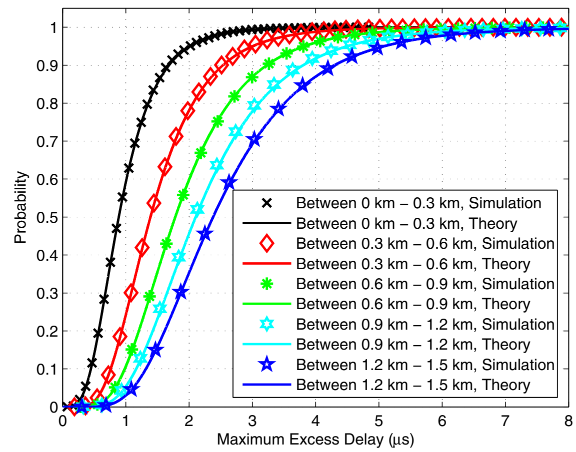

Fig. 3: CDF of $T_{\max}$ for the area between consecutive inner circles.

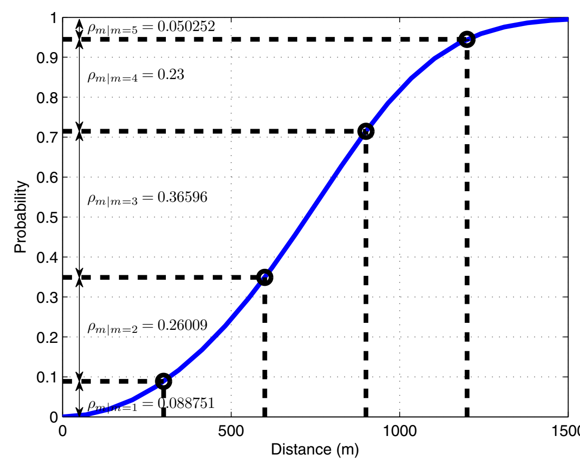

Fig. 4: CDF of r. The probability of having a user between circle with radius of R_m and R_{m-1} also represents ρ_m.

In Fig.3, theoretical and simulation results for CDF of $T_{\max}$ are given for the area between the circles with radius of R_m and R_{m-1}. Monte Carlo simulations match with the closed-form CDF in (6). If $\gamma_{\rm CP}$ is selected 0.95, sufficient $T_{{\rm CP},m|m=1,2,\ldots,5}$ are obtained as $[2,\ 3,\ 3.8,\ 4.5,\ 5.1]$ in μs. Therefore, if the conventional approach is employed for the same range, all OFDMA symbols should have at least $5.1\mu s$ for the cyclic prefix duration for the same $\gamma_{\rm CP}$. In the proposed frame structure, 5 different cyclic prefix durations which are between 2-5.1 μs are used in one frame.

In Fig.4, CDF of r is given using (11) in order to obtain the number of OFDMA symbol with $T_{{\rm CP},m}$ within the frame. The values of $\rho_{m|m=1,2,\ldots,5}$ are obtained approximately as $9\%,\ 26\%,\ 37\%,\ 23\%,\ 5\%]$.

For the mobility model, we consider $p_{\rm road} = 0.4$, $\bar{v}_{\rm city} = 20$ km/h, $\bar{v}_{\rm road} = 70$ km/h, and $\sigma_v = 15$ km/h. Considering $\gamma_{\Delta f} \cong 1$ for $P_{\rm ICI} = -35$ dB, three different Δf_ℓ where $\Delta f_{\ell|\ell=1,2} = [7.5,\ 15,\ 20]$ kHz are determined to employ in the frame. CDF of Δf which satisfies $P_{\rm ICI} = -35$ dB

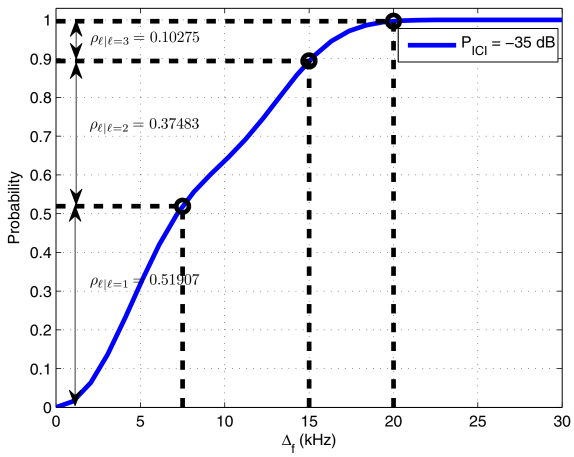

Fig. 5: CDF of Δf which satisfies $P_{\text{ICI}} = -35$ dB upper bound. The y-axis represents the portion of the covered speed variation in the cell.

TABLE I: The number of OFDMA symbols with different cyclic prefix durations and subcarrier spacings within the frame.

$T_{\text{CP},m}{}_{\mid m=1,2,\ldots,5}$	=	$2\mu s$	$3\mu s$	$3.8\mu s$	$4.5\mu s$	$5.1\mu s$
$\Delta f_{\ell\mid\ell=1} = 7.5$ kHz	$\Rightarrow$	7	19	27	17	3
$\Delta f_{\ell\mid\ell=2} = 15$ kHz	$\Rightarrow$	5	13	19	12	3
$\Delta f_{\ell\mid\ell=3} = 20$ kHz	$\Rightarrow$	1	4	5	4	1
$K_{m,\ell}{}_{\mid m=1,2,\ldots,5}$	=	13	36	51	33	7

upper bound is given in Fig.5. Y-axis of CDF curve shows the supported portion of the speed variation in the cell. When the subcarrier spacing is selected as 7.5 kHz, ICI will be less than -35 dB for $v \leq 40$ km/h according to (16). On the other hand, ICI will be less than -35 dB for $v \leq 80$ for $\Delta f = 15$ kHz and $v \leq 105$ km/h for $\Delta f = 20$ kHz. Therefore, $\rho_{\ell|\ell=1,2,3}$ are obtained over calculating the probability of less than 40 km/h, the probability of having between 40 km/h and 80 km/h and the probability of having between 80 km/h and 105 km/h using Fig.5 as $[52\%, \ \%38, \ 10\%]$, respectively. As a result, 52%, 38% and 10% of 140 OFDMA symbols have the same subcarrier spacings of 7.5 kHz, 15 kHz and 20 kHz, respectively. The number of OFDMA symbols with same cyclic prefix size and subcarrier spacings in the frame structure are obtained as in Table I. The increment on the spectral efficiency becomes nearly 5.5% according to (3). In order to compare the increment on the spectral efficiency, the redundancy caused by T_{CP} is around 7% in LTE [12, p. 217].

V. Conclusion

In this paper, a multi-user aware OFDMA frame structure is proposed to exploit the doubly dispersive channels of the users. Multiple cyclic prefix durations and subcarrier spacings are employed in the proposed frame structure. The values of cyclic prefix sizes and subcarrier spacings which will be utilized in one frame are obtained based on a priori knowledge of the statistical characteristics of $T_{\max}$ and the user velocity in the cell. By employing proposed frame structure, nearly %5.5 increment on the spectral efficiency compared to frame structure designed for the worst case scenario is achieved by reducing redundant cyclic prefix usage. At the same time, more frequency spread immune frame structure is obtained.

It is sure that having multiple cyclic prefix durations and subcarrier spacings within the frame impacts the media access control (MAC) layer. While the users are assigned anywhere within the frame in the conventional scheduling, the resource blocks which are suitable for the users are limited in the proposed frame structure. This might impact the flexibility of the MAC protocols. Besides that, the time and frequency spread statistics are required for the proposed structure. The static adaptation with the proposed frame structure might be problematic considering several issues which requires dynamic adaptations. As an extension of this paper, requiring feedback information, dynamic adaptations methods and scheduling which consider the channel quality information can be investigated in order to yield better frame structures.

References

[1] H. Mahmoud, T. Yucek, and H. Arslan, "OFDM for cognitive radio: merits and challenges," *IEEE Wireless Communications*, vol. 16, no. 2, pp. 6–15, Apr. 2009.

[2] S. Sesia, I. Toufik, and M. Baker, *The UMTS Long Term Evolution: From Theory to Practice*. Wiley Publishing, 2009.

[3] J. G. Andrews, A. Ghosh, and R. Muhamed, *Fundamentals of WiMAX: Understanding Broadband Wireless Networking*. Upper Saddle River, NJ, USA: Prentice Hall, 2007.

[4] L. Greenstein, V. Erceg, Y. Yeh, and M. Clark, "A new path-gain/delay-spread propagation model for digital cellular channels," *IEEE Trans. Vehic. Tech.*, vol. 46, no. 2, pp. 477–485, May 1997.

[5] Z. Zhao-yang and L. Li-Feng, "A novel OFDM transmission scheme with length-adaptive cyclic prefix," *Journal of Zhejiang University SCIENCE A*, vol. 5, no. 11, pp. 1336–1342, 2004.

[6] S. D'Alessandro, A. Tonello, and L. Lampe, "Improving WLAN Capacity via OFDMA and Cyclic Prefix Adaptation," in *Proc. IEEE Wireless Days (WD)*, Dec. 2009, pp. 1–5.

[7] ——, "On Power Allocation in Adaptive Cyclic Prefix OFDM," in *Proc. IEEE International Symposium on Power Line Communications and Its Applications (ISPLC)*, Mar. 2010, pp. 183–188.

[8] A. M. Tonello, S. D'Alessandro, and L. Lampe, "Cyclic prefix design and allocation in bit-loaded OFDM over power line communication channels," *IEEE Trans. Commun.*, vol. 58, pp. 3265–3276, Nov. 2010.

[9] Y. Huang and B. Rao, "On Using a Priori Channel Statistics for Cyclic Prefix Optimization in OFDM," in *Proc. IEEE Wireless Communications and Networking Conference (WCNC)*, Mar. 2011, pp. 1460–1465.

[10] S. Das, E. De Carvalho, and R. Prasad, "Dynamically adaptive bandwidth for sub carriers in ofdm based wireless systems," in *Proc. IEEE Wireless Communications and Networking Conference (WCNC)*, Mar. 2007, pp. 1378–1383.

[11] J. S. Wang, S. B. Sim, J. C. Park, J.-S. Um, C. J. Kim, and Y. H. Kim, "Adaptive Resource Allocation for OFDMA with Mixed Frame Structure," in *Proc. IEEE Vehicular Technology Conference (VTC)*, Apr. 2009, pp. 1–5.

[12] D. H. Holma and D. A. Toskala, *LTE for UMTS - OFDMA and SC-FDMA Based Radio Access*. Wiley Publishing, 2009.

[13] V. Erceg, D. Michelson, S. Ghassemzadeh, L. Greenstein, J. Rustako, A.J., P. Guerlain, M. Dennison, R. Roman, D. Barnickel, S. Wang, and R. Miller, "A model for the multipath delay profile of fixed wireless channels," *IEEE Journal on Selected Areas in Communications*, vol. 17, no. 3, pp. 399–410, Mar. 1999.

[14] A. Sahin, E. Guvenkaya, and H. Arslan, "User distance distribution for overlapping and coexisting cell scenarios," *Accepted to IEEE Wireless Comm. Letters*, 2012.

[15] T. Rappaport, *Wireless Communications: Principles and Practice*, 2nd ed. Upper Saddle River, NJ, USA: Prentice Hall, 2001.

[16] C. Bettstetter, H. Hartenstein, and X. Pérez-Costa, "Stochastic properties of the random waypoint mobility model," *Wireless Networks*, vol. 10, pp. 555–567, Sep. 2004.

[17] P. Bratanov and E. Bonek, "Mobility model of vehicle-borne terminals in urban cellular systems," *IEEE Trans. Vehic. Tech.*, vol. 52, no. 4, pp. 947–952, Jul. 2003.

[18] P. Dintchev, B. Perez-Quiles, and E. Bonek, "An improved mobility model for 2G and 3G cellular systems," *Proc. IEE International Conference on 3G Mobile Communication Technologies*, vol. 1, pp. 402–406, 2004.

[19] G. Paschos, E. Vagenas, and S. Kotsopoulos, "User Mobility Model Based on Street Pattern," in *Proc. IEEE Vehicular Technology Conference (VTC)*, vol. 4, May 2005, pp. 2123–2126.

[20] D. Shnidman, "The calculation of the probability of detection and the generalized Marcum Q-function," *IEEE Transactions on Information Theory*, vol. 35, no. 2, pp. 389–400, Mar. 1989.

[21] Y. Li and J. Cimini, L.J., "Bounds on the interchannel interference of OFDM in time-varying impairments," *IEEE Trans. Commun.*, vol. 49, no. 3, pp. 401–404, Mar. 2001.

[22] 3GPP TS 36.814 V9.0.0, "Evolved Universal Terrestrial Radio Access (E-UTRA); Further advancements for E-UTRA physical layer aspects V9.0.0," Mar. 2010.